

DMD #24489

The Effect of Breast Cancer Resistance Protein (Bcrp) and P-glycoprotein (Mdr1a/1b) on the Brain Penetration of Flavopiridol, Gleevec, Prazosin and PF-407288 in Mice

Lin Zhou, Kari Schmidt, Frederick R. Nelson, Veronica Zelesky, Matthew D. Troutman, and Bo Feng

Department of Pharmacokinetics, Dynamics, and Drug Metabolism, Pfizer Global Research and Development, Groton, Connecticut (K.S., F.R.N., V.Z., M.D.T., B.F.); and Department of Pharmaceutics, University of Washington, Seattle, Washington (L.Z.)

DMD #24489

Running title: Function of Bcrp and P-gp on brain penetration of drugs in mice

Address correspondence to:

Bo Feng, Ph.D.

Pfizer Inc., Eastern Point Road, MS 8118W-131

Groton, CT 06340

Phone: 860-715-2756, email: bo.feng2@pfizer.com

Number of text pages (including references): 35

Number of tables: 5

Number of figures: 3

Number of references: 29

Number of words in the abstract: 250

Number of words in the introduction: 806

Number of words in the discussion: 2660

ABBREVIATIONS: ABCB1/MDR1/Mdr1, multidrug resistance protein; P-gp, P-glycoprotein; ABCG2/BCRP/Bcrp, breast cancer resistance protein; BBB, blood-brain barrier; P_{app} , apparent permeability; HEK 293, human embryonic kidney 293 cells; MDCK, Madine-Darby canine kidney; WT, wild-type; KO, knockout; LC-MS/MS, liquid chromatography-tandem mass spectrometry; ER, efflux ratio; RR, ratio of ratios; A, apical; B, basolateral; PK, pharmacokinetics.

DMD #24489

Abstract:

The role of breast cancer resistance protein (Bcrp) and the combined activities of Bcrp and P-glycoprotein (P-gp, Mdr1a/1b) in limiting the brain penetration of drugs at blood-brain barrier (BBB) were investigated using wild-type FVB, Mdr1a/1b^(-/-, -/-), Bcrp^(-/-), and Mdr1a/1b^(-/-, -/-)Bcrp^(-/-) mice. Four drugs, flavopiridol, gleevec, PF-407288 and prazosin, with different transport specificity for BCRP/Bcrp and MDR1/Mdr1a were selected, and the drug levels in plasma, cerebrospinal fluid (CSF) and brain of mice were determined. Flavopiridol and prazosin were identified as substrates for both mouse Bcrp and Mdr1a with greater transport associated with Bcrp. The brain/plasma (B/P) ratios at 0.5 and 2 hr in Mdr1a/1b^(-/-, -/-) and Bcrp^(-/-) mice were 1-2-fold for both compounds, while the ratios in Mdr1a/1b^(-/-, -/-)Bcrp^(-/-) mice were more than 5-fold of those observed in FVB mice. Whereas for gleevec, a better substrate of P-gp than Bcrp, the B/P ratios in Bcrp^(-/-) were comparable to those in FVB mice, while the B/P ratios in Mdr1a/1b^(-/-, -/-) and Mdr1a/1b^(-/-, -/-)Bcrp^(-/-) mice were more than 4-fold and 28-fold of those in FVB mice at both time points, respectively. Finally, the Bcrp specific substrate PF-407288 exhibited comparable B/P ratios in Mdr1a/1b^(-/-, -/-) and Bcrp^(-/-) mice, and slightly but significantly increased B/P ratios in Mdr1a/1b^(-/-, -/-)Bcrp^(-/-) mice compared with FVB mice. The B/P ratios of compounds in Mdr1a/1b^(-/-, -/-)Bcrp^(-/-) compared with those in Mdr1a/1b^(-/-, -/-) clearly demonstrate that Bcrp impairs the brain penetration of its substrates. Moreover, P-gp and Bcrp at BBB function synergistically to limit the brain penetration of shared substrates.

DMD #24489

It is widely recognized that the tight junctions between adjacent brain endothelial cells forming the blood-brain barrier (BBB) restrict the entry of compounds by paracellular diffusion from the blood to the brain. Moreover, the transcellular diffusion of compounds through the brain endothelial cells can also be impeded by transmembrane efflux transporters, such as P-glycoprotein (P-gp, MDR1, ABCB1) and breast cancer resistance protein (BCRP, ABCG2). These efflux transporters can eliminate xenobiotics from the brain against a concentration gradient, thereby limiting central nervous system (CNS) exposure to these compounds. Indeed, the prominent effect of P-gp at BBB is well established, and P-gp is functionally important in limiting the brain penetration of its substrates (Schinkel et al., 1994; Chen et al., 2003; Scherrmann, 2005). Like P-gp, BCRP is another major member of the ABC family of drug transporters, highly expressed in BBB as well. BCRP has been found at the luminal side of human brain capillary endothelial cells (Cooray et al., 2002) and the mRNA level of mouse analog *Bcrp* was ~700 times more in brain microvessels than in the cortex of the mice (Cisternino et al., 2004), implying that mouse *Bcrp* may play a key role at the BBB. BCRP has been identified to accept sulfoconjugated organic anions as well as hydrophobic and amphiphilic compounds (Lee et al., 2005) and the substrate specificity has considerable, but varying, overlaps with that of P-gp (Doyle and Ross, 2003). To date, the importance of BCRP in the disposition of drugs has been demonstrated in various studies (Allen et al., 1999; Jonker et al., 2002; Kruijtz et al., 2002; Lee et al., 2005; Zaher et al., 2006). However, the relevance of this transporter to the CNS distribution of drugs is not well understood. It has been reported that brain penetration of imatinib increased 4.2-fold in mice pretreated with elacridar, an inhibitor of both *Bcrp* and P-gp (Breedveld et al., 2005).

DMD #24489

Consistently, imatinib brain penetration has been observed to increase 2.5-fold in Bcrp^(-/-) mice (Breedveld et al., 2005), demonstrating that Bcrp restricts its substrates across mouse brain *in vivo*. The Cisternino group has also demonstrated that brain uptake of two mouse Bcrp substrates, mitoxantrone and prazosin, increased ~3-fold and ~2-fold, respectively, in Mdr1a/1b^(-/-, -/-) mice in the presence of elacridar, confirming that Bcrp plays a role in limiting brain penetration of drugs (Cisternino et al., 2004). In contrast, Lee et al. reported that mitoxantrone and dehydroepiandrosterone sulfate (DHEAS) brain uptake did not change in Bcrp^(-/-) mice, although mitoxantrone brain uptake increased ~1.6-fold in Mdr1a/1b^(-/-, -/-) mice in the presence of elacridar (Lee et al., 2005), thus leading these authors to conclude that Bcrp may not be important in limiting brain penetration of its substrates. Additionally, another group has reported the K_p value (C_{brain}/C_{plasma}) did not change for Bcrp substrates, 2-amino-1-methyl-6-phenylimidazo[4,5-b]pyridine (van Herwaarden et al., 2003) and 2-amino-3-methylimidazo[4,5-f]quinoline (van Herwaarden et al., 2003; van Herwaarden et al., 2006) in Bcrp^(-/-) vs. wild-type (WT) mice. Despite efforts devoted to investigate the role which BCRP/Bcrp plays *in vivo* in relation to brain penetration, the significance is still unclear in mice and human.

In the present study, we conducted studies in Mdr1a/1b^(-/-, -/-), Bcrp^(-/-), and Mdr1a/1b^(-/-, -/-)Bcrp^(-/-) knockout (KO) mice to gain understanding of the *in vivo* role of Bcrp and the combined role of Bcrp and P-gp in brain penetration. Previous studies have mainly utilized inhibitors of the Bcrp transporter to explicate the *in vivo* functions of Bcrp expressed in BBB. However, the inhibitors may not be Bcrp specific and the inhibition may not be complete at the plasma concentrations achieved, thus potentially complicating

DMD #24489

the results and conclusions. Importantly, we highlight the great value of Mdr1a/1b^(-/-, -/-) Bcrp^(-/-) in this work so that there is no potential compensatory up-regulation of P-gp or Bcrp in this triple KO mice, which could confound the attempts to assess the functions of two transporters at the BBB. Additionally, *in vitro* – *in vivo* relationships around BCRP efflux liability are typically assumed to be analogous to those derived for P-gp, but have yet to be explicitly studied. This work includes studies to further appreciate the following two aims: a) the *in vivo* role of Bcrp efflux and the combined role of Bcrp and P-gp in influencing CNS distribution of its substrates; and b) how *in vitro* metrics around BCRP/Bcrp can be used to predict *in vivo* effect. For the *in vitro* profiling, BCRP/Bcrp and MDR1/Mdr1a efflux liability of our selected compounds were tested using the relevant transporter transfected MDCK cells. Subsequently, the pharmacokinetics (PK) (Johne et al.), including brain penetration of a subset of the compounds were determined in FVB WT, Mdr1a/1b^(-/-, -/-), Bcrp^(-/-), and Mdr1a/1b^(-/-, -/-) Bcrp^(-/-) KO mice. Finally, the results of these studies were compared to assess the effect of Bcrp at the BBB, in attempts to establish a correlation between the *in vitro* transporter assay and the *in vivo* effects.

DMD #24489

Material and Methods

Materials. Flavopiridol, gleevec, PF-407288 and prazosin were obtained from Pfizer Inc (Groton, CT). High-performance liquid chromatography (HPLC) grade dimethyl sulfoxide (DMSO) was obtained from Fisher Scientific Co. (Pittsburgh, PA), and used as the solvent for making stock solutions for all compounds. MEM alpha medium, penicillin-streptomycin, FBS, nonessential amino acids, L-glutamine, trypsin-EDTA, phosphate-buffered saline (PBS), buffer B (Hanks balanced salt solution with 25 mM D-glucose, 20 mM HEPES, 1.25 mM CaCl_2 and 0.5 mM MgCl_2), and Geneticin were purchased from Invitrogen (Carlsbad, CA). Feeder trays and BD 96-well membrane inserts were purchased from Becton Dickinson BioScience (San Jose, CA), and 1.2 mL 96-well deep well plates were purchased from Marsh (Rochester, NY). Mouse plasma (Cat# 35142-2) and brain (Cat# 55004-2) was purchased from Pel-Freeze (Rogers, AR).

Cell Culture. MDCK cells were obtained from ATCC (Rockville, MD). The MDR1 transfected MDCK cell line (MDR1-MDCK) was acquired externally (Dr. Piet Borst, Netherlands Cancer Institute, Amsterdam, The Netherlands), mouse *Mdr1a* transfected MDCK (*Mdr1a*-MDCK) and human BCRP transfected MDCK (BCRP-MDCK) were generated by Pfizer Inc (Xiao et al., 2006). Mouse TREx-Bcrp-MDCK, which uses the Tet-inducible promoter to express the mouse *Bcrp*, was acquired through a collaboration with XenoPort (Santa Clara, CA). All cell lines, except the TREx-Bcrp-MDCK cell line, were grown and maintained in MEM supplemented with 10% FBS, 2 mM L-glutamine, 100 units/mL penicillin, 100 $\mu\text{g/mL}$ streptomycin, and 0.5 mg/mL G418 at 37°C in a 5% CO_2 incubator. As an inducible cell line, the TREx-Bcrp-MDCK cells were grown and maintained as other cells except that G418 was omitted in the

DMD #24489

culture medium and 1 $\mu\text{g/mL}$ Doxycycline was added for induction. Cells were grown to 80–90% confluence and treated with trypsin-EDTA prior to harvesting for subculturing or for further use in transwell assays.

Transporter 96-well Transwell Assays. A similar high throughput 96-well transwell assay method was used, as described previously (Feng et al., 2007). On day 1, MDCK, human MDR1-MDCK, mouse Mdr1a-MDCK, human BCRP-MDCK and mouse TReX-Bcrp-MDCK cells were seeded at a cell density of 2.5×10^5 cells/ml in complete MEM alpha media on either side of the PET membrane of 96-well inserts. For apical (A) to basolateral (B) (A>B) transport studies, cells were seeded into the A side of the insert, while for B>A transport studies, cells were seeded onto the underside of the membrane when the insert was placed upside-down. The inserts for B>A transport were incubated for 60 min at 37°C, 95% humidity and 5% CO₂ to allow the attachment of cells on the membrane. Then, all the inserts were placed into feeder trays containing 37 mL of complete MEM alpha growth media, and cultured (37°C, 95% humidity and 5% CO₂) for 5 days.

All in vitro transport experiments were performed under sink conditions (at least 90% or greater of mass applied to the donor compartment remained over the course of the experiment). For both A>B and B>A transport, the donor is the A compartment and the receiver is the B compartment, because in plates used for B>A transport, cells were seeded on the other side of the insert membrane. This experimental approach allows for a self-correction of non-specific binding when efflux ratios are calculated. On day 5, medium was removed from the insert and 75 μL of fresh buffer B containing test substrates at 2 μM was added using a 96-well pipettor (Apricot Designs, CA). Later the

DMD #24489

insert was placed into a 96-well collection plate containing 250 μ L of buffer B per well and then incubated at 37°C, 95% humidity and 5% CO₂. After 2 hr and half (within the linear flux region), 150 μ L was removed from each well of the collection plate and transferred to a fresh 96-well deep well plate. The remaining 100 μ L of buffer B in the collection plate was removed and replaced with 100 μ L of acetonitrile containing an internal standard. After mixing, 60 μ L of acetonitrile was removed and added to the 150 μ L buffer B sample previously removed.

Transport Study Sample Analysis by LC-MS/MS. The samples were centrifuged for 10 min at 3500 rpm in a Sorvall RC 3C Plus centrifuge (Sorvall Products L.P., Newtown, CT) prior to LC-MS/MS analysis. The samples were analyzed using a Sciex API-4000 triple quadrupole mass spectrometer (PE Sciex, Ontario, ON, Canada) equipped with a turbo ion source (ESI) interface. Gilson 215 autosampler (Gilson Instruments, Middleton, WI) was used to make 25 μ l injections with further sample concentration and on-line cleanup achieved through the use of a single column/valve-switching system equipped with a two-position 10-port Valco valve (Valco Instruments, Houston, TX) and a cartridge-style 1.5 x 5 mm column (Optimize Technologies Inc., Oregon City, OR) custom packed with 13 μ m particle size Showa Denko (Tokyo, Japan) ODP polymeric packing material. Two Shimadzu SCL-10AD VP HPLC pumps (Shimadzu Inc., Torrance, CA) were used to deliver mobile phase at a flow rate of 1.2 mL/min. Aqueous mobile phase (sample loading) consisted of 95% 2 mM ammonium acetate / 5% 50:50 acetonitrile/methanol and organic mobile phase (sample elution) consisted of 10% 2 mM ammonium acetate / 90% 50:50 acetonitrile/methanol. Data acquisition was carried out in positive ionization mode (ion spray voltage of 5.5 kV) for

DMD #24489

prazosin, gleevec and flavopiridol and in negative mode (ion spray voltage of 4.5 kV) for PF-407288. Selected reaction monitoring was used to monitor for analyte and internal standard simultaneously. The following transitions were used for analyte detection: 384.5 m/z → 247 m/z for prazosin, 495 m/z → 395 m/z for gleevec, 402.8 m/z → 340.6 m/z for flavopiridol and 381 m/z → 119 m/z for PF-407288. For internal standard PF-628374, a transition of 687.3 m/z → 319.7 m/z was used in positive mode and 685 m/z → 366 m/z in negative mode. A Q2 offset voltage of 5V was used with collision energies of 45 eV for prazosin and PF-40728800 and 30 eV for gleevec and flavopiridol.

Transwell Data Analysis. The following procedures were used to determine compound apparent permeability (P_{app}) values for studies conducted with MDCK, MDR1-MDCK, mouse Mdr1a-MDCK, BCRP-MDCK and mouse TReX-Bcrp-MDCK cell lines.

The P_{app} was calculated using eq. 1:

$$P_{app} = \frac{1}{Area * C_D(0)} * \frac{dM_r}{dt} \quad 1$$

where Area is the surface area of the cell monolayer (0.0625 cm²), $C_D(0)$ is the initial concentration of compound applied to the donor chamber, t is time, M_r is the mass of compound appearing in the receiver compartment as a function of time, and dM_r/dt is the flux of the compound across the cell monolayer. The efflux ratio (ER) was calculated using eq. 2:

$$ER = \frac{P_{app,B>A}}{P_{app,A>B}} \quad 2$$

DMD #24489

Where A>B and B>A denote transport direction in which P_{app} was determined. The ratio of ratios (RR) was calculated using equation 3:

$$RR = \frac{ER_{transfected}}{ER_{wt}} \quad 3$$

where $ER_{transfected}$ is the ER determined in the transfected MDCK cells (MDR1-MDCK, Mdr1a-MDCK, BCRP-MDCK and TREx-Bcrp-MDCK) and ER_{wt} is the ER determined in WT MDCK cells. RR_{MDR1} , RR_{Mdr1a} , RR_{BCRP} and RR_{Bcrp} denote RR determined for ER in MDR1-MDCK, Mdr1a-MDCK, BCRP-MDCK and TREx-Bcrp-MDCK transfected cells, respectively, compared with ER in WT MDCK.

Animal Studies. Male WT FVB, Mdr1a/1b^(-/-, -/-), Bcrp^(-/-), and Mdr1a/1b^(-/-, -/-) Bcrp^(-/-) mice of approximately 8 weeks of age, weighing 25 to 30 g, were obtained from Taconic Farms (Germantown, NY). Upon arrival, the mice were maintained for at least 5 days on a 12 hr light/dark cycle in a temperature- and humidity-controlled environment with free access to food and water. The mice were housed in clear polycarbonate boxes (n = 5 per box) containing sawdust. The study was conducted in accordance with approved Pfizer Animal Care and Use Procedures.

Dose Administration and Sample Collection. Mice were administered a single 5 mg/kg subcutaneous dose (n = 4-5 per genotype per time point per drug). Dosing solutions of each drug were prepared in PBS, with or without 5% DMSO or 10% glycerol formal, when necessary; or 20% hydroxypropyl β -cyclodextrin. The resulting doses were administered at a dose in a volume of 10 mL/kg. Mice were euthanized in a CO₂ chamber at 0.5 and 2 hr post-dose. Whole blood was collected by cardiac puncture into Microtainer tubes containing lithium heparin and stored on ice until centrifuged for the

DMD #24489

preparation of plasma. CSF was collected via puncture of the cisterna magna using a 25 gauge needle attached to polyethylene tubing (internal diameter of 2.0 mm) and a syringe. Whole brains were collected by decapitation, rinsed with PBS and weighed. CSF and whole brains were immediately frozen on dry ice upon collection until analysis.

Animal Sample Preparation. In preparation for analysis by LC-MS/MS, brain tissue was diluted 1:4 (w:v) with PBS and homogenized with a Mini Beadbeater (Biospec Products, Inc, Bartlesville, OK) with 2 mm zirconia beads for 2 min. For all of the drugs, the brain and plasma samples were treated in a similar manner in terms of analysis. The samples were processed through deproteinization using acetonitrile containing an internal standard that was structurally similar to each individual analyte. The CSF samples were directly injected on to the LC-MS/MS system.

Animal Study Sample Analysis Using LC-MS/MS. The samples were analyzed using a Micromass Quattro Ultima LC-MS/MS system (Waters Corporation, Milford MA). A leap autosampler (Gilson Instruments, Middleton, WI) was used to make 10 μ L injections. Separation of the compound and corresponding internal standard was achieved using a Phenomenex Luna C18 (2) column (2 x 30 mm; 5- μ particle size). Two Shimadzu HPLC pumps (Shimadzu Inc., Torrance, CA) were used to deliver mobile phase at a flow rate of 0.6 mL/min. Aqueous mobile phase (Phase A) consisted of 20 mM ammonium acetate with the addition of 0.1% formic acid and 0.1% isopropanol. The organic mobile phase (Phase B) was 100% acetonitrile. During the first half-minute of the chromatographic run, the mobile phase solvents were held at a constant ratio 95:5 (A:B) that was followed by a 1.3 min linear gradient to a mobile phase solvent ratio of 10:90 (A:B). The intermediate condition was held for 0.2 min followed by an immediate return

DMD #24489

to the starting conditions. The starting conditions were then maintained for a one-minute period of re-equilibration. Data acquisition was carried out in positive ionization mode and the instrument was fitted with an electrospray ionization Z-spray interface for all compounds. Selected reaction monitoring was used to monitor for analyte and internal standard simultaneously. The following transitions were used for analyte detection: 384.0 m/z \rightarrow 247.0 m/z for prazosin, 494.2 m/z \rightarrow 394.2 m/z for gleevec, 402.0 m/z \rightarrow 341.2 m/z for flavoperidol and 382.0 m/z \rightarrow 186.0 m/z for PF-407288. For internal standard detection, the following transitions were used: 414.1 m/z \rightarrow 249 m/z for CP-018857, 416.1 m/z \rightarrow 139.1 m/z for CP-660551, 366.1 m/z \rightarrow 281 m/z for CE-267266 and 438.2 m/z \rightarrow 216.1 m/z for PF-548939. The collision energy values for prazosin, gleevec, flavopiridol and PF-407288 were 25, 30, 22 and 25 eV, respectively.

Animal Study Data and Statistical Analysis. The experiments were set up as a randomized complete block design with genotype as the main effect and time as a secondary effect. The sampling times were 0.5 and 2 hr postdose. The genotypes included WT, Mdr1a/1b^(-/-, -/-), Bcrp^(-/-), and Mdr1a/1b^(-/-, -/-)Bcrp^(-/-) KO. The sample size was determined assuming a small percentage of dropouts for a significance level of 0.05 and a power of 0.8 at each time point. The comparisons of concentrations and ratios were done using a student's *t* test with unequal variances.

Brain Tissue and Plasma Protein Binding Studies. Plasma and brain free fraction values were determined for all compounds through the use of a 96-well equilibrium dialysis apparatus (HTDialysis, Gales Ferry, CT). Mouse plasma and brains were obtained from a commercial source. The mouse brains were diluted at a ratio of 1:2 (w:v) with PBS followed by homogenization via the Mini Beadbeater (Biospec Products,

DMD #24489

Inc.) with 2 mm zirconia beads for 2 min. Spectra-Por number 2 membranes with molecular weight cutoff of 12-14 kDa were used for equilibrium dialysis and were purchased from Spectrum Laboratories (Rancho Dominguez, CA). Prior to the experiments, membranes were sequentially soaked in HPLC grade water for 15 min, 30% ethanol for 15 min, rinsed with HPLC grade water and then stored in PBS until use.

The pH of the plasma, brain homogenate and buffer was adjusted to 7.4 with either 20% phosphoric acid or 5 N NaOH. Compounds at the specific concentrations were spiked into plasma, brain homogenate and buffer and 150 μ L were then loaded into the dialysis apparatus and dialyzed against an equal amount of PBS. The plate was sealed with a CO₂ permeable adhesive membrane and equilibrium was achieved over a 6 h incubation period in a Stericult cell incubator at 37°C, 95% humidity and 5% CO₂. Following the conclusion of the incubation, 100 μ L of the donor, receiver and equilibrium controls were transferred to marsh tubes containing an equal amount of the alternate matrix to yield an identical matrix between the donor and receiver samples from each incubation. The mixed matrix samples were immediately frozen and stored at -20°C until analysis. Samples were analyzed using LC-MS/MS conditions described above for *in vivo* studies.

The unbound fraction f_u was calculated using the following equation:

$$f_u = \frac{1/D}{((1/f_{u2}) - 1) + 1/D}$$

where D is the dilution factor for biological matrix and f_{u2} is the unbound fraction measured from diluted samples.

DMD #24489

Results

Compounds Selection Using *In Vitro* 96-well Transporter Transwell Assay.

Transport studies performed in a 96-well transwell format were employed to identify human MDR1, mouse Mdr1a, human BCRP and mouse Bcrp substrates using MDCK, human MDR1-MDCK, mouse Mdr1a-MDCK, human BCRP-MDCK, and mouse TReX-Bcrp-MDCK cell lines. Four compounds out of more than 30 compounds tested, including PF-407288 (Fig. 1), flavopiridol, prazosin and gleevec, were chosen for further evaluation in the transporter knockout (KO) mouse models. The P_{app} and ER values determined using MDCK, MDR1-MDCK, Mdr1a-MDCK, BCRP-MDCK and TReX-Bcrp-MDCK transwell assays are illustrated in Table 1. The magnitude of RR values were employed to definitively assign whether a compound was a human MDR1 substrate, and the same approach was used to identify human BCRP, mouse Mdr1a and mouse Bcrp substrates (Feng, et al., 2008). A previously established cutoff of 1.7 for RR_{MDR1} and 1.5 for RR_{Mdr1a} , RR_{BCRP} and RR_{Bcrp} has been shown to yield a positive *in vitro* and *in vivo* correlation for human and mouse MDR1/Mdr1a and BCRP/Bcrp substrates (Xiao et al., 2006; Feng et al., 2008). The RR_{MDR1} , RR_{Mdr1a} , RR_{BCRP} and RR_{Bcrp} for the four compounds can be found in Table 2, and our qualitative assessment of substrate specificity and preference is based on respective magnitude of RR values. Based on the cutoffs, PF-407288 was identified as a human and mouse BCRP/Bcrp specific substrate. Flavopiridol and prazosin were categorized as MDR1/Mdr1a and BCRP/Bcrp dual substrates, though they appear to be more strongly associated with BCRP/Bcrp transport per their higher RR_{BCRP} and RR_{Bcrp} vs. RR_{MDR1} and RR_{Mdr1a} values. Whereas, gleevec was recognized as a MDR1/Mdr1a and BCRP/Bcrp common substrate as well, but appears to

DMD #24489

be a more effective MDR1/Mdr1a substrate with larger RR_{MDR1} and RR_{Mdr1a} compared with RR_{BCRP} and RR_{Bcrp} .

***In vivo* PK of Flavopiridol, Gleevec, PF-407288 and Prazosin in transporter KO Mice Models.** To determine the individual and combined role of Bcrp and Mdr1a/1b in the CNS penetration of drugs in mice, the systemic and central exposures of PF-407288, flavopiridol, prazosin and gleevec were determined in Mdr1a/1b^(-/-, -/-), Bcrp^(-/-), and Mdr1a/1b^(-/-, -/-)Bcrp^(-/-) KO mice as well as the WT FVB strain. The compounds were administrated at 5 mg/kg subcutaneous dose and concentrations were determined in plasma, brain and CSF samples obtained at 0.5 and 2 hr postdose (Fig. 2). Concentrations in plasma and brain samples were all at quantifiable levels, while the concentrations in CSF were not detectable in all samples (e.g., CSF concentrations of PF-407288 at 0.5 and 2 hr postdose were only detectable in Mdr1a/1b^(-/-, -/-)Bcrp^(-/-) mice).

Additionally, the B/P ratios for all four compounds in Mdr1a/1b^(-/-, -/-), Bcrp^(-/-), and Mdr1a/1b^(-/-, -/-)Bcrp^(-/-) mice as well as in FVB were calculated (Table 3). To measure the effects of functional impairment of Bcrp or/and Mdr1a/1b on the brain penetration of drugs, the concentrations of four compounds in brain, plasma and CSF as well as B/P ratios, from Mdr1a/1b^(-/-, -/-), Bcrp^(-/-), and Mdr1a/1b^(-/-, -/-)Bcrp^(-/-) mice vs. FVB mice at both 0.5 and 2 hr time points were summarized in Table 4. There were 2- to 50-fold increases in the brain concentrations of four compounds in Mdr1a/1b^(-/-, -/-)Bcrp^(-/-) mice compared with FVB mice at both time points. Consistently, the CSF concentrations increased 2- to 15-fold in Mdr1a/1b^(-/-, -/-)Bcrp^(-/-) mice vs. FVB mice for all four compounds at both time points as well (Table 4). Interestingly, the brain and CSF

DMD #24489

increases of the four compounds in Mdr1a/1b^(-/-, -/-) and Bcrp^(-/-) were not comparable with the increases in Mdr1a/1b^(-/-, -/-)Bcrp^(-/-) mice. For gleevec, there was a 3- to 4-fold increase of brain concentrations in Mdr1a/1b^(-/-, -/-) mice and no increase of brain concentrations in Bcrp^(-/-) mice, but 19- to 50-fold increase of brain concentration in Mdr1a/1b^(-/-, -/-)Bcrp^(-/-) mice as compared with those determined in FVB mice at both 0.5 and 2 hr. Also, for flavopiridol and prazosin, the brain concentrations increased considerably in both Mdr1a/1b^(-/-, -/-) and Bcrp^(-/-) mice, but to a much lower extent than the increases observed in Mdr1a/1b^(-/-, -/-)Bcrp^(-/-) mice in comparison to the FVB mice. Slightly different from the other three compounds, PF-407288 showed no appreciable increase of the brain concentrations in Mdr1a/1b^(-/-, -/-) and Bcrp^(-/-) mice as compared to the FVB mice, but there were more than 2-fold increases in Mdr1a/1b^(-/-, -/-)Bcrp^(-/-) mice vs. FVB mice. Consistently, the CSF concentration increases for the four compounds in Mdr1a/1b^(-/-, -/-)Bcrp^(-/-) mice were at much larger extent than the CSF concentration increases in Mdr1a/1b^(-/-, -/-) and Bcrp^(-/-) mice as compared to the FVB mice (Table 4). On the other hand, the plasma concentrations of four compounds were comparable in Mdr1a/1b^(-/-, -/-), Bcrp^(-/-) and Mdr1a/1b^(-/-, -/-)Bcrp^(-/-) mice compared with FVB mice, except prazosin with higher plasma concentrations in three types of KO mice vs. FVB mice (P<0.01) at the 2 hr time point, suggesting the potential attenuation of some transporter-mediated clearance mechanisms for prazosin in KO mice. Although the mechanism is not clear and will require further investigation, it is noted that the changes of plasma concentrations were not comparable with the changes of brain and CSF concentrations.

DMD #24489

Furthermore, the B/P ratios for all four compounds in four types of mice (Table 3), and B/P ratios in $Mdr1a/1b^{(-/-, -/-)}$, $Bcrp^{(-/-)}$, and $Mdr1a/1b^{(-/-, -/-)}Bcrp^{(-/-)}$ mice compared with those in FVB were calculated (Table 4). Consistent with the increases in brain, the increases of B/P ratios in $Mdr1a/1b^{(-/-, -/-)}Bcrp^{(-/-)}$ mice were tremendous, but those in the respective $Mdr1a/1b^{(-/-, -/-)}$, and $Bcrp^{(-/-)}$ mice were to a much lower extent.

Unbound Tissue Exposures. To account for the differences in the various compounds' affinity for brain tissue and plasma, the unbound fraction in plasma and brain were experimentally calculated for the four compounds (Table 5). Free brain and free plasma concentrations at 0.5 hr and 2 hr were determined using the $f_{u,brain}$ and $f_{u,plasma}$, respectively, and free B/P and CSF/P ratios at 0.5 hr and 2 hr postdose are presented in Fig. 3. Consistent with the increase of total B/P ratios in $Mdr1a/1b^{(-/-, -/-)}Bcrp^{(-/-)}$ mice compared with FVB mice, the free B/P ratios showed commensurate increases in $Mdr1a/1b^{(-/-, -/-)}Bcrp^{(-/-)}$ mice vs. FVB mice for all four compounds. Whereas, the free B/P increases in $Mdr1a/1b^{(-/-, -/-)}$ and $Bcrp^{(-/-)}$ were not as dramatic as those in $Mdr1a/1b^{(-/-, -/-)}Bcrp^{(-/-)}$ mice. For both flavopiridol and prazosin, the free B/P ratios of $Mdr1a/1b^{(-/-, -/-)}$ and $Bcrp^{(-/-)}$ vs. FVB were modestly higher, however, free B/P ratios of $Mdr1a/1b^{(-/-, -/-)}Bcrp^{(-/-)}$ mice vs. FVB increased dramatically (Fig. 3). For gleevec, although the free B/P ratios of $Bcrp^{(-/-)}$ vs. FVB were comparable (P, not significant) and free B/P ratios of $Mdr1a/1b^{(-/-, -/-)}$ vs. FVB increased significantly ($P < 0.05$), free B/P ratios of $Mdr1a/1b^{(-/-, -/-)}Bcrp^{(-/-)}$ vs. FVB mice dramatically increased ($P < 0.01$). In the case of PF-407288, the free B/P ratios of $Bcrp^{(-/-)}$ and $Mdr1a/1b^{(-/-, -/-)}$ vs. FVB mice were equivalent, while the free B/P ratio of $Mdr1a/1b^{(-/-, -/-)}Bcrp^{(-/-)}$ mice was modestly and significantly ($P < 0.05$) higher than that in FVB. Similar to the increases of free B/P ratios

DMD #24489

in Bcrp^(-/-), Mdr1a/1b^(-/-, -/-) and Mdr1a/1b^(-/-, -/-)Bcrp^(-/-) vs. FVB mice, an alternate metric used to assess brain penetration, free CSF/P ratios, showed similar enhanced increases in Mdr1a/1b^(-/-, -/-)Bcrp^(-/-) compared with the increases in Bcrp^(-/-) and Mdr1a/1b^(-/-, -/-) mice (Fig. 3).

DMD #24489

Discussion

More than 30 commercial compounds have been tested using *in vitro* transporter studies to identify MDR1/Mdr1a and BCRP/Bcrp substrates that could be utilized in later *in vivo* experiments to understand the respective roles of Bcrp and Mdr1a/b in affecting brain penetration. BCRP/Bcrp specific substrates were believed to be ideal compounds for elucidating the *in vivo* role of Bcrp at BBB, because the prevalence of P-gp in determining brain penetration may cause P-gp to conceal the effect of BCRP in the case of dual substrates. However, due to the overlapping substrate specificities between MDR1/Mdr1a and BCRP/Bcrp, only one compound, PF-407288, was classified as a BCRP/Bcrp specific substrate with RR_{MDR1} , RR_{Mdr1a} , RR_{BCRP} and RR_{Bcrp} of 1.1, 1.1, 6.9 and 3.7, respectively, after screening more than 30 commercial compounds and thousands of Pfizer compounds. PF-407288 is a Pfizer proprietary compound for the treatment in diabetes target (Fig. 1). The other three selected compounds, flavopiridol, prazosin and gleevec, were chosen to display various transport characteristics for BCRP/Bcrp and MDR1/Mdr1a, with the hope that the contribution of the two major efflux transporters at BBB would be clearly weighed out. Regarding transport characteristics, flavopiridol exhibited RR_{MDR1} , RR_{Mdr1a} , RR_{BCRP} and RR_{Bcrp} of 3.1, 3.0, 6.0 and 8.2, respectively. Thus, flavopiridol was categorized as being transported more effectively by BCRP/Bcrp than MDR1/Mdr1a. The *in vitro* transport specificities for prazosin were similar to flavopiridol, with RR_{MDR1} , RR_{Mdr1a} , RR_{BCRP} and RR_{Bcrp} of 2.1, 2.3, 4.3 and 8.5, respectively. In contrast to flavopiridol and prazosin, gleevec was classified as a more effective MDR1/Mdr1a substrate, with RR_{MDR1} , RR_{Mdr1a} , RR_{BCRP} and RR_{Bcrp} of 4.7, 4.0, 2.4 and 2.3, respectively. Interestingly, the four compounds, as well as the other tested

DMD #24489

compounds, exhibited similar transport specificities between human and mouse for both P-gp and BCRP. This observation is consistent with our previous report that species differences for P-gp substrate specificity and resulting transport activity is minimal between human and mouse (Feng et al., 2008), and this appears to hold true for BCRP/Bcrp as well.

With different transport specificities, the four compounds could help us establish the overall contribution of Mdr1a/1b and Bcrp to the brain penetration in mice. Another important criterion for compound selection for *in vivo* studies was the compound permeability. The passive permeability of four compounds were assessed in MDCK parent cell line (Table 1), and as we reported previously, $P_{app,A>B}$ is able to reflect the compounds' permeability *in vivo* (Feng et al., 2008). Based on the $P_{app,A>B}$ values in MDCK cells and comparison with known permeability standards, flavopiridol, prozasin and PF-407288 had good passive permeabilities with $P_{app,A>B}$ values in MDCK higher than 10×10^{-6} cm/s. Although gleevec had a moderate permeability with $P_{app,A>B}$ values in MDCK of 3.9×10^{-6} cm/s, the brain penetration of gleevec has been successfully measured previously in Mdr1a/1b^(-/-, -/-) and Bcrp^(-/-) mice (Breedveld et al., 2005; Bihorel et al., 2007). Additionally, all four compounds displayed similar physico-chemical properties for typical CNS drugs (Pajouhesh H, 2005), including molecular weight less than 400, polar surface area (PSA) higher than 90 Å, reasonable plasma binding ($f_u \geq 3\%$) and good metabolic stability. Taking the MDCK $P_{app,A>B}$ and physico-chemical properties into account, all four compounds were believed to be able to readily cross the BBB by passive permeability, and were deemed suitable for *in vivo* CNS disposition studies.

DMD #24489

First, for the BCRP/Bcrp specific substrate, PF-407288, the brain concentrations were slightly increased in Bcrp^(-/-) and Mdr1a/1b^(-/-, -/-) vs. FVB mice, whereas the brain concentrations in Mdr1a/1b^(-/-)Bcrp^(-/-) mice vs. FVB was significantly enhanced by more than 2-fold ($P < 0.01$) at both 0.5 and 2 hr (Fig. 2 & Table 4). Moreover, the CSF concentrations of PF-407288 were not detectable in FVB, Mdr1a/1b^(-/-, -/-) and Bcrp^(-/-) mice, whereas the CSF concentrations in Mdr1a/1b^(-/-, -/-)Bcrp^(-/-) were detectable at both time points (Fig. 2). The B/P ratios of PF-407288 in Mdr1a/1b^(-/-, -/-), Bcrp^(-/-) and Mdr1a/1b^(-/-, -/-)Bcrp^(-/-) mice were slightly higher than FVB (Table 3). Surprisingly, the brain concentrations were not considerably increased in Bcrp^(-/-) mice vs. FVB mice although PF-407288 was identified as a specific Bcrp substrate *in vitro*. It is very likely that Bcrp affected brain penetration of PF-407288 in mice to a lower extent than what we expected from the *in vitro* transport activities. It seems that efflux transporters at BBB must counteract the brain penetration of PF-407288, but Bcrp may not be the only one involved, particularly as B/P ratios generated in Bcrp^(-/-) mice, as well as in other KO mice, were much less than one indicating some additional barriers to brain penetration of PF-407288. Collectively, although *in vitro* transporter assay results classified PF-407288 as a Bcrp substrate, Bcrp does not appear to be a major factor leading to its poor brain penetration in mice. No dramatic brain concentrations and B/P ratios increase in Bcrp^(-/-) and Mdr1a/1b^(-/-, -/-)Bcrp^(-/-) mice against FVB were observed. It is reasonable to conclude that Bcrp impeded CNS disposition of PF-407288, but to a small extent.

Compounds in the second group are common substrates for both MDR1/Mdr1a and BCRP/Bcrp, including flavopiridol and prazosin. The brain concentrations for both compounds exhibited increases in Bcrp^(-/-) and Mdr1a/1b^(-/-, -/-) mice compared with FVB

DMD #24489

mice, with more enhancement in Mdr1a/1b^(-/-, -/-) against Bcrp^(-/-) mice (Fig. 2 and Table 4). Likewise the B/P ratios had a larger increase in Mdr1a/1b^(-/-, -/-) compared with those determined in Bcrp^(-/-) mice as well (Table 3). This was different from what we may have predicted based on the *in vitro* transport activities, given that the two compounds were demonstrated to be weaker Mdr1a substrates compared with Bcrp *in vitro*. The reason for this disconnect could be due to the higher expression of Mdr1a/1b in mouse BBB compared with that of Bcrp, and/or the compounds' different affinities to Mdr1a/1b vs. Bcrp. Although based on mRNA level, Mdr1a expression is slightly higher than Bcrp in mouse brain homogenate (Lee et al., 2005), Mdr1a expression could be much higher than Bcrp at mouse BBB since Mdr1a is more enriched than Bcrp in BBB compared with those in brain homogenate (12-fold vs. 5.6-fold) (Lee et al., 2005). Pfizer internal data has also confirmed Mdr1a expression is higher than Bcrp at mouse BBB (manuscript submitted). Consequently, the impact of functional impairment of Bcrp on the brain penetration of Bcrp and P-gp shared substrates likely becomes smaller than predicted from the *in vitro* Bcrp transport activities. Additionally, Sugiyama group recently observed that the brain penetration of common substrates of Bcrp and P-gp exhibited a smaller increase in Bcrp^(-/-) mice than expected from the *in vitro* Bcrp activities, and proposed that the effect of functional impairment of Bcrp could be modulated by P-gp activity on their shared substrates (Enokizono et al., 2008).

Surprisingly, for flavopiridol and prazosin, the B/P in Mdr1a/1b^(-/-, -/-)Bcrp^(-/-) mice increased dramatically compared with that observed in FVB (more than 5-fold, Table 4). Obviously, the increases in B/P ratios in Mdr1a/1b^(-/-, -/-)Bcrp^(-/-) mice are much higher than the simple addition of increases of B/P ratios in Bcrp^(-/-) and Mdr1a/1b^(-/-, -/-)

DMD #24489

compared with FVB. This finding was confirmed by pharmacodynamic observations around prazosin's hypnotic side effects. The triple KO mice became inactive shortly following dose administration, and did not return to the initial active status at 2 hr postdose, while Bcrp^(-/-) or Mdr1a/1b^(-/-, -/-) mice became inactive ~10 min after dosing and came back to normal at around 1 hr postdose. The FVB strain did not show any apparent change in activity. These all support the hypothesis that the two transporters act in concert (synergistically and/or in a compensatory fashion), not additively, to limit the brain penetration of dual substrates. Interestingly, Kusuhara and Sugiyama proposed an explanation for the observed synergism of efflux transporters at the BBB in Mdr1a/1b^(-/-, -/-)Bcrp^(-/-) mice recently by providing a conceptual basis describing the synergism and its ramifications for kinetics (Kusuhara and Sugiyama, 2009). When both P-gp- and Bcrp-mediated transport are significantly greater than the passive diffusion, the remaining efflux in Bcrp^(-/-) or Mdr1a/1b^(-/-, -/-) mice will prevent a marked reduction in the luminal efflux clearance. Whereas, in Mdr1a/1b^(-/-, -/-)Bcrp^(-/-) mice, no efflux remains and the synergism is therefore observed. The kinetic concept of this apparent synergism was illustrated in Sugiyama's paper. Alternatively, it is important to note the transporter expression differences in the KO mice may produce this apparent compensation in brain impairment for Mdr1a/1b^(-/-, -/-) and Bcrp^(-/-) vs. WT mice. Of interest, it has been claimed that there was ~3 times more Bcrp mRNA in the microvessels from P-gp-deficient mutant mouse brains than in the microvessels of WT mouse brains (Cisternino et al., 2004). Collectively, the compensatory higher expression of Bcrp in Mdr1a/1b^(-/-, -/-) mice could mitigate B/P increases of flavopiridol and prazosin in Mdr1a/1b^(-/-, -/-) mice to be not as dramatic as expected. Similarly, it would be reasonable to postulate that Mdr1a/1b is up-

DMD #24489

regulated in Bcrp^(-/-) mice, since P-gp and Bcrp are two major efflux transporters in mouse BBB to protect brain from xenobiotics. If the up-regulation occurs in both cases, the increases of B/P in Bcrp^(-/-) compared with FVB could greatly underestimate the contribution of Bcrp in brain penetration of dual substrates by virtue of compensation by Mdr1a/1b. With no confounding possibility of up-regulation, the B/P ratio increases in Mdr1a/1b^(-/-, -/-)Bcrp^(-/-) mice could serve to reflect the real overall contribution of both transporters in the brain penetration of shared substrates *in vivo*. Moreover, that B/P increases in Mdr1a/1b^(-/-, -/-)Bcrp^(-/-) mice were significantly higher than those in Mdr1a/1b^(-/-, -/-) (P<0.01) compared with FVB mice at both time points (Table 3 & 4) clearly demonstrate the effect of Bcrp on the brain penetration of flavopiridol and prazosin. If we assume that Bcrp does not contribute to the brain penetration of its substrate, the increases of B/P ratios in Mdr1a/1b^(-/-, -/-)Bcrp^(-/-) mice should be comparable to that in Mdr1a/1b^(-/-, -/-) mice, even with the up-regulation of Bcrp in Mdr1a/1b^(-/-, -/-) mice. Clearly, Bcrp must contribute to the brain penetration of flavopiridol and prazosin.

Regarding the last compound gleevec, *in vitro* transport studies indicated that gleevec was preferentially transported by Mdr1a than Bcrp. The B/P ratios in Bcrp^(-/-) and Mdr1a/1b^(-/-, -/-) mice compared with FVB were ~1-fold and ~4-fold, respectively (Table 4), which implied that Mdr1a/1b accounts for limitation of the brain penetration of gleevec. It is likely that Mdr1a/1b could offset the deletion of Bcrp and maintain the B/P ratios in Bcrp^(-/-) and WT at a similar low level. This is consistent with the previous reports suggesting that P-gp plays a more important role than Bcrp in limiting the distribution of gleevec to the brain (Hamada et al., 2003; Breedveld et al., 2005; Bihorel et al., 2007). However, the remarkable increase of B/P ratios in Mdr1a/1b^(-/-, -/-)Bcrp^(-/-)

DMD #24489

mice vs. B/P ratios in Mdr1a/1b^(-/-, -/-) mice with ~7-fold at 0.5 hr and ~14-fold at 2 hr (Table 3) suggests that Bcrp must contribute to the brain penetration of gleevec as well but to a much lower extent than P-gp does. Up-regulation of the other efflux transporters in the Bcrp^(-/-) or Mdr1a/1b^(-/-, -/-) mice could also explain the lower B/P increases in Bcrp^(-/-) and Mdr1a/1b^(-/-, -/-) mice than expected based on the extrapolation of the *in vitro* transport activities.

In CNS drug discovery, K_p (B/P) is the most commonly used parameter to evaluate brain penetration (Pardridge, 2004), but its relevance has been occasionally questioned. In a recent study at Pfizer, K_p was determined for a set of the 32 most prescribed CNS drugs and ranged from 0.1 to 24 in mice (Doran et al., 2005). However, a compound having a K_p value as low as 0.1, such as sulpiride, can still be a successful CNS drug, suggesting that it is difficult to assess brain penetration based upon K_p alone (Doran et al., 2005). $K_{p, \text{ free}}$, defined as the ratio of free brain and free plasma concentration at equilibrium, has been identified as a better parameter to assess brain penetration (Maurer et al., 2005; Syvanen et al., 2006). Thus, it is essential to understand the impact of the binding in plasma and brain towards brain penetration. Unbound fractions in mouse brain and plasma were determined for all four compounds (Table 5), and free B/P and CSF/free plasma ratios at 0.5 hr and 2 hr are presented in Fig. 3. For the four compounds, the $f_{u, \text{ brain}}$ and $f_{u, \text{ plasma}}$ for each compound are within a couple of folds. Thus, the free B/P concurs with total B/P for these four compounds as shown in Table 3. Consequently, B/P ratios are valuable parameters to evaluate brain penetration for the four compounds, as discussed earlier. Also, CSF/free plasma ratios correlated well with free B/P (Fig. 3), suggesting that CSF is a good indicator of free brain exposure for

DMD #24489

the four compounds. As mentioned before, free B/P is used to assess a potential brain impairment of compounds in CNS drug discovery, and free B/P around 1 (within 3-fold errors) will suggest that the compounds have no potential brain impairment issues (Maurer et al., 2005). Since the free B/P ratios for flavopiridol, prazosin and gleevec in $Mdr1a/1b^{(-/-, -/-)}Bcrp^{(-/-)}$ were close to 1 at 2 hr with lower free B/P ratios at 0.5 hr (Fig. 3), the data suggest that distribution of the three compounds between brain and plasma was delayed at 0.5 hr, and it is expected that there will be no brain impairment for the three compounds at 2 hr and longer time points. However, it should be noted that the free B/P ratios for PF-407288 were not close to a unity, even in the triple KO mice, which further implies that other efflux transporters besides P-gp and Bcrp could contribute to the brain impairment of PF-407288 in mice.

These studies unambiguously indicate that Bcrp is an important component at the mouse BBB that can impede brain penetration, and Bcrp and $Mdr1a/1b$ likely work in synergy or in a compensatory fashion to limit CNS distribution of their shared substrates across BBB in mice. Recent work from the van Tellingen group has also demonstrated this mechanism of Bcrp and P-gp at mouse BBB (de Vries et al., 2007). Compared with the prominent role of P-gp at the mouse BBB, our results suggest that Bcrp appears to contribute less than P-gp to the brain penetration of dual substrates. Certainly, the effect of Bcrp may differ among substrates, and thus the effects may be greater or lesser for any particular drug. However, our study provides definitive evidences that Bcrp is functional at the mouse BBB. It is also important to remember besides P-gp and Bcrp, other efflux transporters, such as MRP4, are highly expressed at mouse BBB (Leggas et al., 2004), and could contribute to the brain penetration of drugs across BBB *in vivo*.

DMD #24489

Regarding *in vitro* - *in vivo* correlation, we have established a good correlation between *in vitro* efflux ratios in human MDR1-MDCK and mouse Mdr1a-MDCK with *in vivo* brain penetration based on K_p values (Doran et al., 2005; Feng et al., 2008), whereas a positive relationship between the *in vitro* and *in vivo* Bcrp activities has not yet been established. These studies suggest a positive relationship between the *in vitro* Bcrp transport activities and the *in vivo* CNS penetration of Bcrp substrates. Thus, *in vitro* efflux ratios in Bcrp transport assays could help predict *in vivo* relevance of Bcrp at BBB.

Overall, knowledge of how Bcrp mediates drug transport at the BBB *in vivo* could provide important information on the mechanisms underlying drug transport across BBB and CNS toxicity and importantly, our findings show that P-gp alone is sometimes insufficient to understand the role of efflux transport in brain penetration particularly for dual substrates. Our study underlines that BCRP is also a crucial component at BBB which may cause the brain impairment of CNS drugs. We conclude that it is more effective to use the triple KO mice rather than P-gp or Bcrp KO mice alone to study the brain penetration of their substrates drugs, and to understand the overall contributions of these two efflux transporters in prediction of clinical relevance.

DMD #24489

Acknowledgements

The authors would like to thank Mr. Ralph Davidson for his help in transwell assays, and Ms. Julie Cianfroga for her help in animal studies.

DMD #24489

References

Allen JD, Brinkhuis RF, Wijnholds J and Schinkel AH (1999) The mouse Bcrp1/Mxr/Abcp gene: amplification and overexpression in cell lines selected for resistance to topotecan, mitoxantrone, or doxorubicin. *Cancer Res* **59**:4237-4241.

Bihorel S, Camenisch G, Lemaire M and Scherrmann JM (2007) Influence of breast cancer resistance protein (Abcg2) and p-glycoprotein (Abcb1a) on the transport of imatinib mesylate (Gleevec) across the mouse blood-brain barrier. *J Neurochem* **102**:1749-1757.

Breedveld P, Pluim D, Cipriani G, Wielinga P, van Tellingen O, Schinkel AH and Schellens JH (2005) The effect of Bcrp1 (Abcg2) on the in vivo pharmacokinetics and brain penetration of imatinib mesylate (Gleevec): implications for the use of breast cancer resistance protein and P-glycoprotein inhibitors to enable the brain penetration of imatinib in patients. *Cancer Res* **65**:2577-2582.

Chen C, Hanson E, Watson JW and Lee JS (2003) P-glycoprotein limits the brain penetration of nonsedating but not sedating H1-antagonists. *Drug Metab Dispos* **31**:312-318.

Cisternino S, Mercier C, Bourasset F, Roux F and Scherrmann JM (2004) Expression, up-regulation, and transport activity of the multidrug-resistance protein Abcg2 at the mouse blood-brain barrier. *Cancer Res* **64**:3296-3301.

DMD #24489

Cooray HC, Blackmore CG, Maskell L and Barrand MA (2002) Localisation of breast cancer resistance protein in microvessel endothelium of human brain. *Neuroreport* **13**:2059-2063.

de Vries NA, Zhao J, Kroon E, Buckle T, Beijnen JH and van Tellingen O (2007) P-glycoprotein and breast cancer resistance protein: two dominant transporters working together in limiting the brain penetration of topotecan. *Clin Cancer Res* **13**:6440-6449.

Doran A, Obach RS, Smith BJ, Hosea NA, Becker S, Callegari E, Chen C, Chen X, Choo E, Cianfroga J, Cox LM, Gibbs JP, Gibbs MA, Hatch H, Hop CE, Kasman IN, Laperle J, Liu J, Liu X, Logman M, Maclin D, Nedza FM, Nelson F, Olson E, Rahematpura S, Raunig D, Rogers S, Schmidt K, Spracklin DK, Szewc M, Troutman M, Tseng E, Tu M, Van Deusen JW, Venkatakrishnan K, Walens G, Wang EQ, Wong D, Yasgar AS and Zhang C (2005) The impact of P-glycoprotein on the disposition of drugs targeted for indications of the central nervous system: evaluation using the MDR1A/1B knockout mouse model. *Drug Metab Dispos* **33**:165-174.

Doyle LA and Ross DD (2003) Multidrug resistance mediated by the breast cancer resistance protein BCRP (ABCG2). *Oncogene* **22**:7340-7358.

DMD #24489

Enokizono J, Kusuvara H, Ose A, Schinkel AH and Sugiyama Y (2008) Quantitative investigation of the role of breast cancer resistance protein (Bcrp/Abcg2) in limiting brain and testis penetration of xenobiotic compounds. *Drug Metab Dispos* **36**:995-1002.

Feng B, Mills JB, Davidson RE, Mireles RJ, Janiszewski JS, Troutman MD and de Moraes SM (2008) In vitro P-glycoprotein assays to predict the in vivo interactions of P-glycoprotein with drugs in the central nervous system. *Drug Metab Dispos* **36**:268-275.

Hamada A, Miyano H, Watanabe H and Saito H (2003) Interaction of imatinib mesilate with human P-glycoprotein. *J Pharmacol Exp Ther* **307**:824-828.

Johne A, Kopke K, Gerloff T, Mai I, Rietbrock S, Meisel C, Hoffmeyer S, Kerb R, Fromm MF, Brinkmann U, Eichelbaum M, Brockmoller J, Cascorbi I and Roots I (2002) Modulation of steady-state kinetics of digoxin by haplotypes of the P-glycoprotein MDR1 gene. *Clin Pharmacol Ther* **72**:584-594.

Jonker JW, Buitelaar M, Wagenaar E, Van Der Valk MA, Scheffer GL, Scheper RJ, Plosch T, Kuipers F, Elferink RP, Rosing H, Beijnen JH and Schinkel AH (2002) The breast cancer resistance protein protects against a major chlorophyll-derived dietary phototoxin and protoporphyria. *Proc Natl Acad Sci U S A* **99**:15649-15654.

Kruijtzter CM, Beijnen JH, Rosing H, ten Bokkel Huinink WW, Schot M, Jewell RC, Paul EM and Schellens JH (2002) Increased oral bioavailability of topotecan in

DMD #24489

combination with the breast cancer resistance protein and P-glycoprotein inhibitor GF120918. *J Clin Oncol* **20**:2943-2950.

Kusuhara H and Sugiyama Y (2009) In vitro-in vivo extrapolation of transporter-mediated clearance in the liver and kidney. *Drug Metab Pharmacokinet* Manuscript accepted.

Lee YJ, Kusuhara H, Jonker JW, Schinkel AH and Sugiyama Y (2005) Investigation of efflux transport of dehydroepiandrosterone sulfate and mitoxantrone at the mouse blood-brain barrier: a minor role of breast cancer resistance protein. *J Pharmacol Exp Ther* **312**:44-52.

Leggas M, Adachi M, Scheffer GL, Sun D, Wielinga P, Du G, Mercer KE, Zhuang Y, panetta JC, Johnston B, et al. (2004) Mrp4 confers resistance to topotecan and protects the brain from chemotherapy. *Mol Cell Bio* **24**:7612-7621.

Maurer TS, Debartolo DB, Tess DA and Scott DO (2005) Relationship between exposure and nonspecific binding of thirty-three central nervous system drugs in mice. *Drug Metab Dispos* **33**:175-181.

Pajouhesh H LG (2005) Medicinal chemical properties of successful central nervous system drugs. *NeuroRX: the Journal of the American Society for Experimental NeuroTherapeutics* **2**:541-553.

DMD #24489

Pardridge WM (2004) Holy grails and in vitro blood-brain barrier models. *Drug Discov Today* **9**:258.

Scherrmann JM (2005) Expression and function of multidrug resistance transporters at the blood-brain barriers. *Expert Opin Drug Metab Toxicol* **1**:233-246.

Schinkel AH, Smit JJ, van Tellingen O, Beijnen JH, Wagenaar E, van Deemter L, Mol CA, van der Valk MA, Robanus-Maandag EC, te Riele HP and et al. (1994) Disruption of the mouse *mdr1a* P-glycoprotein gene leads to a deficiency in the blood-brain barrier and to increased sensitivity to drugs. *Cell* **77**:491-502.

Syvanen S, Xie R, Sahin S and Hammarlund-Udenaes M (2006) Pharmacokinetic consequences of active drug efflux at the blood-brain barrier. *Pharm Res* **23**:705-717.

van Herwaarden AE, Jonker JW, Wagenaar E, Brinkhuis RF, Schellens JH, Beijnen JH and Schinkel AH (2003) The breast cancer resistance protein (Bcrp1/Abcg2) restricts exposure to the dietary carcinogen 2-amino-1-methyl-6-phenylimidazo[4,5-b]pyridine. *Cancer Res* **63**:6447-6452.

van Herwaarden AE, Wagenaar E, Karnekamp B, Merino G, Jonker JW and Schinkel AH (2006) Breast cancer resistance protein (Bcrp1/Abcg2) reduces systemic exposure of the

DMD #24489

dietary carcinogens aflatoxin B1, IQ and Trp-P-1 but also mediates their secretion into breast milk. *Carcinogenesis* **27**:123-130.

Xiao Y, Davidson R, Smith A, Pereira D, Zhao S, Soglia J, Gebhard D, de Morais S and Duignan DB (2006) A 96-well efflux assay to identify ABCG2 substrates using a stably transfected MDCK II cell line. *Mol Pharm* **3**:45-54.

Zaher H, Khan AA, Palandra J, Brayman TG, Yu L and Ware JA (2006) Breast cancer resistance protein (Bcrp/abcg2) is a major determinant of sulfasalazine absorption and elimination in the mouse. *Mol Pharm* **3**:55-61.

DMD #24489

Figure Legends

Fig. 1. Chemical structure of PF-407288.

Fig. 2. Brain, plasma, and CSF concentration-time profiles for flavopiridol (a), gleevec (b), PF-407288 (c) and prazosin (d) in FVB (o), Bcrp^(-/-) (♦), Mdr1a/1b^(-/-, -/-) (▲), and Bcrp^(-/-)Mdr1a1b^(-/-, -/-) (■) mice between 0.5 hr and 2 hr following subcutaneous administration (5 mg/kg). Data points represent mean ± SD values from 3-5 male mice.

Fig. 3. Free brain/free plasma and CSF/free plasma ratios for flavopiridol (a), gleevec (b), PF-407288 (c) and prazosin (d) in four types of mice (FVB, solid black; Bcrp^(-/-), striped; Mdr1a/1b^(-/-, -/-), dotted; and Bcrp^(-/-)Mdr1a1b^(-/-, -/-), blank) at 0.5 hr and 2 hr after subcutaneous administration (5mg/Kg). Data points represent mean ± SD values from 3-5 male mice. *: vs. FVB, p<0.05, and **: vs. FVB, p<0.01

TABLE 1

Summary of mean Papp values ($\times 10^{-6}$ cm/s) and efflux ratios for compounds tested in transwell assay^c

	Flavopiridol					Gleevec					PF-407288					Prazosin				
	A>B		B>A		ER ^d	A>B		B>A		ER ^d	A>B		B>A		ER ^d	A>B		B>A		ER ^d
	Mean	SD	Mean	SD		Mean	SD	Mean	SD		Mean	SD	Mean	SD		Mean	SD	Mean	SD	
MDCK ^a	16.6	3.1	14.1	2.0	0.9	3.9	0.4	15.5	2.0	4.0	13.6	2.9	9.8	3.1	0.7	11.0	2.0	21.3	3.9	1.9
MDR1 ^a	10.6	2.8	29.3	3.9	2.8	1.3	0.2	23.9	3.7	18.9	9.8	2.7	7.8	2.1	0.8	6.8	1.9	27.3	4.8	4.0
Mdr1a ^a	13.5	1.4	36.7	4.7	2.7	1.9	0.5	30.9	5.0	16.1	10.7	1.1	8.4	1.7	0.8	8.6	1.0	37.7	11.3	4.4
BCRP ^a	9.4	1.1	51.0	8.0	5.4	3.7	1.7	34.6	2.5	9.4	4.4	0.5	21.0	5.9	4.8	4.9	1.0	39.5	2.0	8.1
Bcrp U ^b	18.2	2.1	23.7	9.7	1.3	15.7	4.1	24.4	2.2	1.6	11.2	0.4	20.2	3.9	1.8	22.7	8.5	32.4	10.9	1.4
Bcrp I ^b	4.0	4.4	42.9	1.3	10.7	10.1	2.0	36.6	3.9	3.6	3.4	0.7	22.8	0.8	6.7	6.5	0.8	77.8	3.1	11.9

^aHuman MDR1, mouse Mdr1a and human BCRP substrate properties were examined in the MDCK cell line stably transfected with MDR1, Mdr1a or BCRP genes, respectively.

^bMouse Bcrp substrate properties were examined in the MDCK cell line transfected with inducible Bcrp genes. U: un-induce Bcrp, I: induced Bcrp

^cData for all compounds were from 3-4 individual experiments, except the data for flavopiridol in inducible Bcrp cells are presented as the average of two individual experiments.

^dER: efflux ratio, which was equal to B>A *Papp* divided by A>B *Papp* in different cell lines.

TABLE 2

Summary of ratio of efflux ratios for compounds tested in transwell assay^a

Compounds	RR _{MDR1}	RR _{Mdr1a}	RR _{BCRP}	RR _{Bcrp}
Flavopiridol	3.1	3.0	6.0	8.2
Gleevec	4.7	4.0	2.4	2.3
PF-407288	1.1	1.1	6.9	3.7
Prazosin	2.1	2.3	4.3	8.5

^aRR_{MDR1} equals ER_{MDR1}/ER_{MDCK}, RR_{Mdr1a} equals ER_{Mdr1a}/ER_{MDCK}, RR_{BCRP} equals ER_{BCRP}/ER_{MDCK}, and RR_{Bcrp} equals ER_{Bcrp}/ER_{Bcrp} U.

TABLE 3

Total B/P at 0.5 and 2 hr for compounds in FVB, Mdr1a/1b^(-/-, -/-), Bcrp^(-/-) and Mdr1a/1b^(-/-, -/-)Bcrp^(-/-) mice after subcutaneous administration^a.

	FVB	Mdr1a/1b ^(-/-, -/-)	Bcrp ^(-/-)	Mdr1a/1b ^(-/-, -/-) Bcrp ^(-/-)
	0.5hr	0.5hr	0.5hr	0.5hr
Flavopiridol	0.42±0.06	0.71±0.07 ^{***}	0.55±0.05 [*]	3.11±0.59 ^{***}
Gleevec	0.02±0.00	0.09±0.02 ^{***}	0.02±0.00	0.58±0.18 ^{**}
PF-407288	0.01±0.001	0.02±0.005 [*]	0.02±0.002 ^{**}	0.03±0.004 ^{**}
Prazosin	0.17±0.01	0.31±0.07 [*]	0.23±0.06	1.04±0.20 ^{**}
	2hr	2hr	2hr	2hr
Flavopiridol	0.92±0.07	1.45±0.39	1.22±0.09 ^{**}	6.34±0.88 ^{***}
Gleevec	0.02±0.00	0.11±0.03 ^{**}	0.02±0.01	1.55±0.77 [*]
PF-407288	0.02±0.003	0.02±0.004	0.02±0.003	0.03±0.004 [*]
Prazosin	0.33±0.03	0.58±0.08 ^{**}	0.37±0.01	1.73±0.26 ^{***}

^aData are presented as mean ± SD from 3-5 male mice. *: vs. FVB, p<0.05; **: vs. FVB, p<0.01; ***: vs. FVB, p<0.001

TABLE 4

Concentration ratios of four compounds at two time points in *Mdr1a/1b*^(-/-, -/-), *Bcrp*^(-/-) and *Mdr1a/1b*^(-/-, -/-)*Bcrp*^(-/-) mice vs. concentrations in FVB mice after subcutaneous administration^a.

	<i>Mdr1a/1b</i> ^(-/-, -/-) vs. FVB				<i>Bcrp</i> ^(-/-) vs. FVB				<i>Mdr1a/1b</i> ^(-/-, -/-) <i>Bcrp</i> ^(-/-) vs. FVB			
	Brain	Plasma	CSF	Brain/Plasma	Brain	Plasma	CSF	Brain/Plasma	Brain	Plasma	CSF	Brain/Plasma
	0.5hr				0.5hr				0.5hr			
Flavopiridol	1.79±0.27	1.06±0.17	1.85±0.21	1.67±0.15	1.42±0.33	1.09±0.28	1.51±0.41	1.29±0.11	10.07±1.87 (***, ###)	1.35±0.12 (*)	5.81±1.56 (**, ##)	7.35±1.41 (**, ##)
Gleevec	3.37±0.35	0.76±0.10	1.54±0.34	4.45±0.79	0.89±0.19	0.94±0.09	1.11±0.41	0.94±0.14	19.03±4.27 (**, ##)	0.69±0.11 (##)	5.80±1.19 (**, ###)	28.23±6.08 (**, ##)
PF-407288	0.98±0.34	0.66±0.20	0.78±0.41	1.53±0.40	1.13±0.33	0.79±0.18	0.45±0.18	1.43±0.14	2.70±0.83 (**, #)	1.34±0.28 (**, ##)	1.88±0.63 (*, ##)	2.02±0.49 (##)
Prazosin	2.26±0.66	1.24±0.33	2.47±1.09	1.86±0.42	1.23±0.09	0.92±0.16	0.83±0.38	1.38±0.32	5.67±0.79 (***, ###)	0.96±0.30	5.24±1.89 (*, ##)	6.14±1.99 (**, ###)
	2hr				2hr				2hr			
Flavopiridol	2.72±1.13	1.92±1.01	4.45±1.82	1.58±0.42	1.86±0.35	1.42±0.34	2.51±0.90	1.33±0.09	16.85±3.40 (***, ###)	2.50±0.68 (#)	15.35±7.25 (*, #)	6.89±0.65 (***, ###)
Gleevec	3.83±1.18	0.90±0.35	N. E.	4.46±1.07	0.84±0.38	0.98±0.31	N. E.	0.86±0.32	50.78±6.96 (***, ###)	0.92±0.36 (#)	N. E.	63.59±11.33 (*, #)
PF-407288	2.10±1.18	1.94±0.65	N. E.	1.02±0.22	1.70±0.26	1.43±0.29	N. E.	1.19±0.17	2.66±0.86	1.93±0.60	N. E.	1.36±0.23 (*)
Prazosin	4.33±1.06	2.42±0.57	1.42±0.10	1.75±0.24	3.62±0.33	3.20±0.36	0.43±0.57	1.10±0.04	22.67±2.25 (***, ###)	4.33±0.73 (**, #)	8.77±3.58 (*, ##)	5.18±0.88 (***, ###)

^aData are presented as mean ± S.D. from 3-5 male mice. N. E.: not estimated.

Comparison of concentration ratios of *Mdr1a/1b*^(-/-, -/-) *Bcrp*^(-/-) vs. FVB and concentration ratios of *Mdr1a/1b*^(-/-, -/-) vs. FVB:

* p<0.05, ** p<0.01, *** p<0.001.

Comparison of concentration ratios of *Mdr1a/1b*^(-/-, -/-) *Bcrp*^(-/-) vs. FVB and concentration ratios of *Bcrp*^(-/-) vs. FVB: # p<0.05, ## p<0.01, ### p<0.001.

TABLE 5

Unbound fractions for four compounds in mouse plasma and mouse brain^a

	$f_{u, \text{plasma}}$	$f_{u, \text{brain}}$
Flavopiridol	0.26±0.03	0.04±0.00
Gleevec	0.09±0.00	0.03±0.01
PF-407288	0.03±0.00	0.07±0.01
Prazosin	0.35±0.03	0.09±0.01

^aData are presented as mean ± SD from three independent determinations.

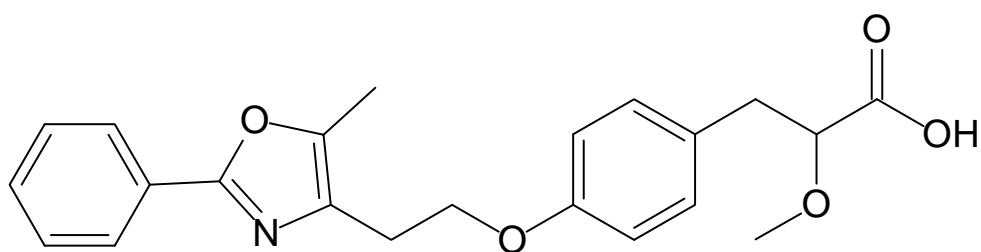
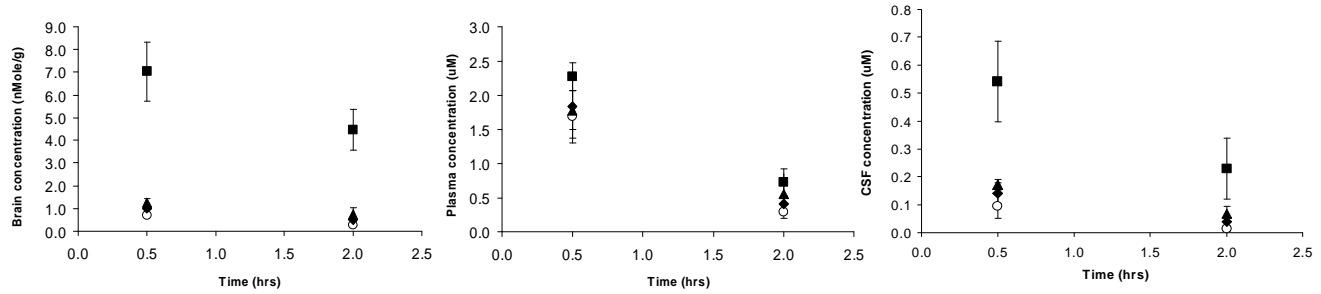
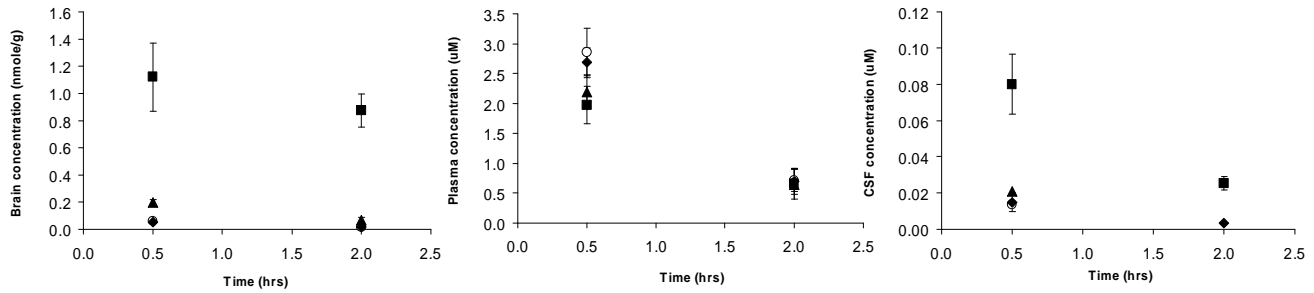


Fig 1

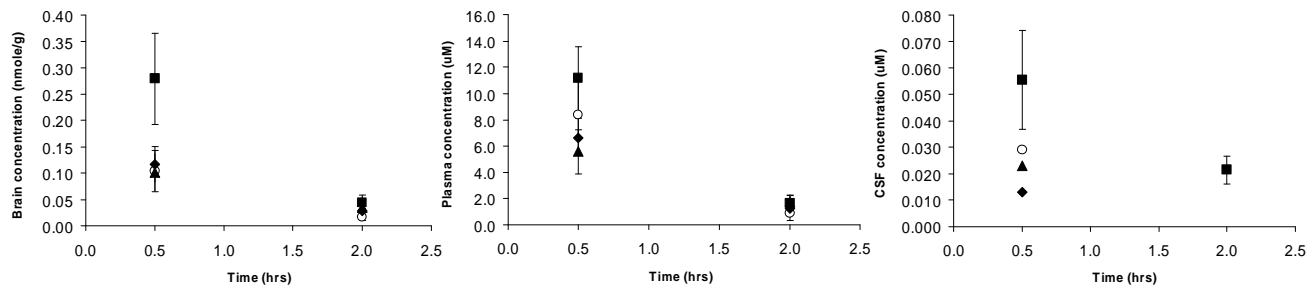
a) Flavopiridol



b) Gleevec



c) PF-407288



d) Prazosin

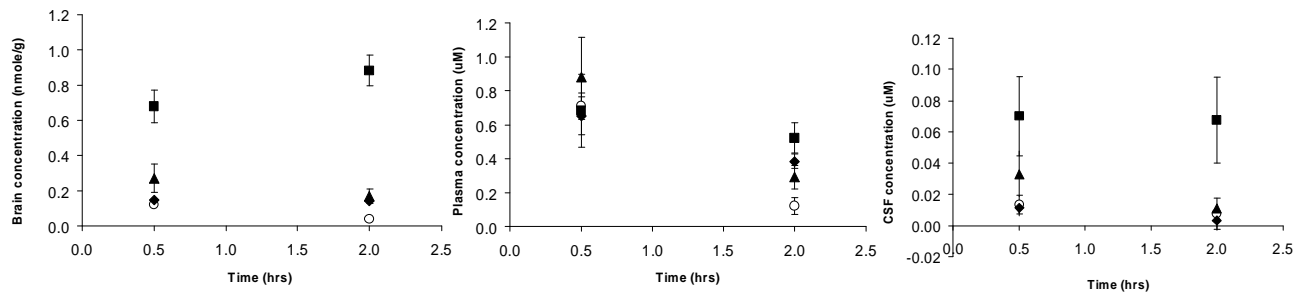
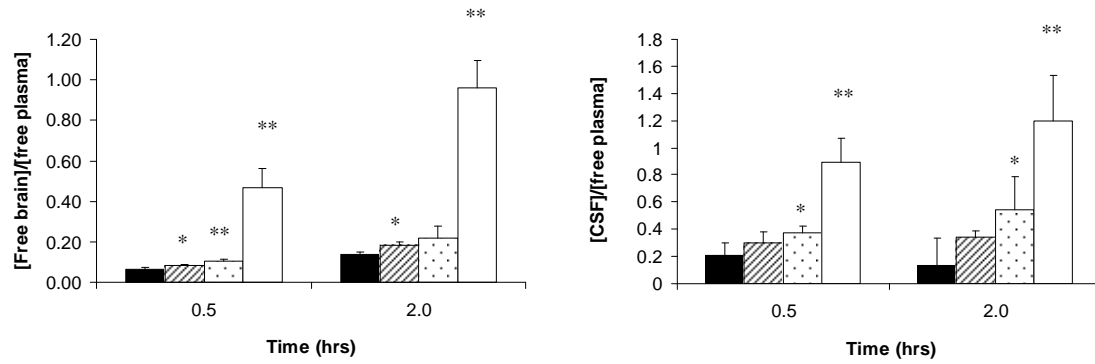
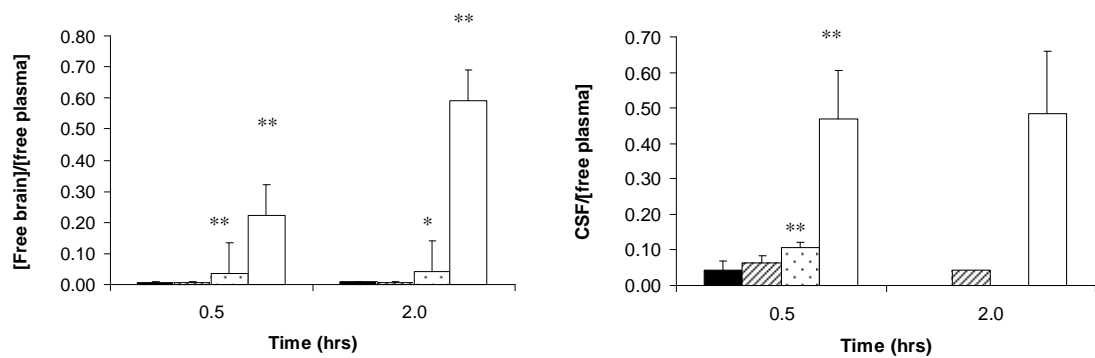


Fig 2

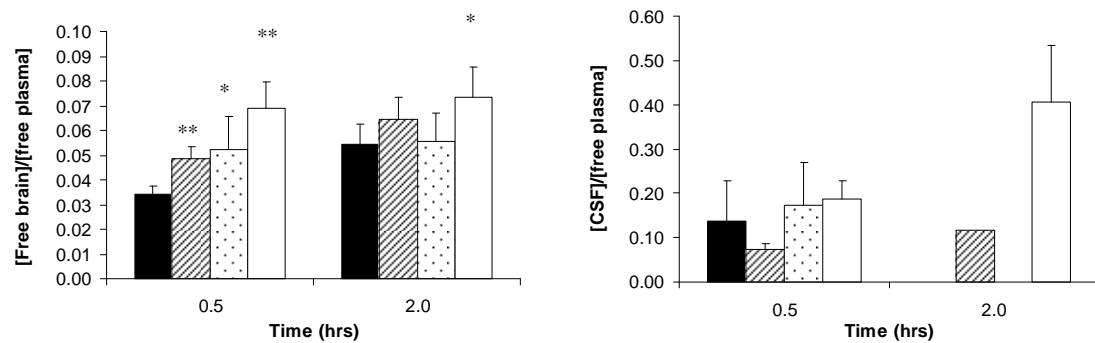
a) Flavopiridol



b) Gleevec



c) PF-407288



d) Prazosin

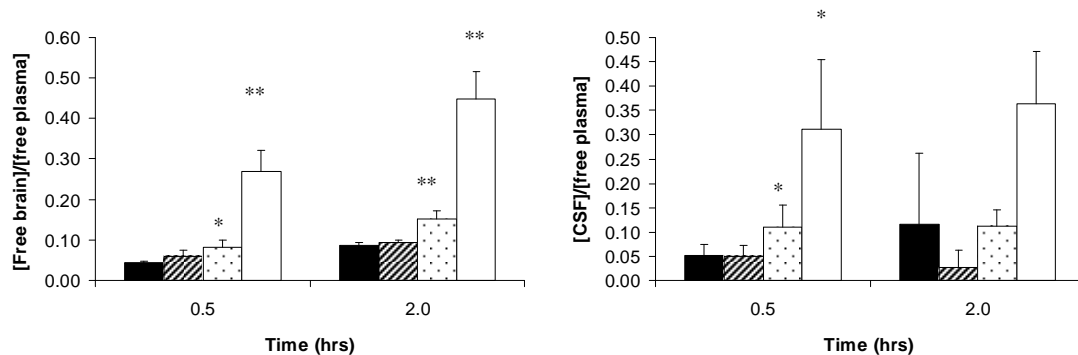


Fig 3